Vol. 79 (1991) ACTA PHYSICA POLONICA A No 1

Proc. XIX International School of Semiconducting Compounds, Jaszowiec 1990

GALLIUM ARSENIDE AND RELATED COMPOUNDS FOR DEVICE APPLICATIONS

J. WOOD,

University of York, Dept of Electronics, Heslington, York YO1 5DD, UK

AND D.V. MORGAN

University of Wales, College of Cardiff, Cardiff, UK

(Received August 8, 1990)

The device applications of gallium arsenide and related III–V compound and alloy semiconductors are reviewed. A range of electronic devices is described, and the current state of the art performance is indicated for each type of device. The devices which will be described are: transferred electron devices – as oscillators up to 200 GHz, GaAs MESFETs – the workhorse microwave solid state device, some monolithic microwave integrated circuit /MMIC/, and heterojunction devices. The use of molecular beam epitaxy MBE to grow III–V semiconductors with great control over the doping, mole fraction of the constituents and the thickness of the epilayer has permitted the construction of devices with atomically abrupt interfaces between regions of different doping and alloy. The electronic devices which make use of such abrupt heterojunctions include: high electron mobility transistors, heterojunction bipolar transistor, and laser diodes. A number of novel devices based on multiple barrier and quantum well structures is also described, including Resonant Tunneling Devices.

PACS numbers: 72.80.Ey, 73.40.Kp, 78.20.Fs

Introduction

Gallium arsenide and related III–V compounds were first investigated as semiconducting materials over thirty years ago. The material properties of these compounds possess some broad similarities with those of that archetypal semiconductor, silicon: they have a similar crystalline structure, and the interatomic bonding is largely covalent [1]. But the III–V compounds were also recognised for

their optical and electronic properties, such as a direct band gap and high electron mobility, that were not found in silicon or germanium. These properties held the promise of new and unique devices such as high efficiency light emitters and light sensors and high speed switching devices, fields where silicon could not readily compete.

The reasons behind these electronic and optical properties, and the consequent interest in gallium arsenide GaAs and similar III–V compounds, lie in the detailed nature of their electron energy band structures. Taking GaAs as typical of III–V semiconductors in which we are interested:

Gallium arsenide has a direct energy band gap. The minimum in the $\varepsilon(k)$ curve in the conduction band lies directly above the maximum in the valence band, in k-space.This allows direct interband recombination of electrons and holes, with the emission of light energy of the appropriate wavelength to the band gap: about 850 nm; no phonon interaction is necessary (Fig. 1). Hence, GaAs is said to be a good optoelectronic material and is used extensively in light-emitting diodes and semiconductor lasers.

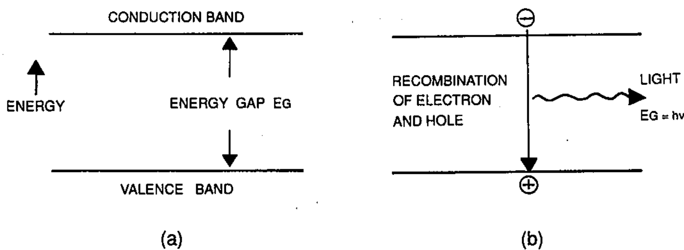

Fig.1. Radiative recombination of electron and hole across a direct band gap E_g.

Gallium arsenide can be made to have a very high resistivity. This is because the band gap of GaAs, 1.43 eV, is relatively large compared to 1.1 eV for silicon. Because of the very strong exponential dependence of the intrinsic carrier density on the bandgap, undoped GaAs has very few intrinsic electrons and holes and hence a high resistivity: it is known as 'semi-insulating' (SI). This allows a simple means of isolating neighbouring devices on an integrated circuit, and eliminates the parasitic capacitances associated with p-n junction isolation methods found in silicon ICs. It is such parasitic elements that degrade device performance at high frequencies. By making GaAs devices on SI substrates, operation at high frequencies can be achieved.

It should be noted that the wide bandgap also gives GaAs superior high temperature performance.

Gallium arsenide has a high electron mobility. At low electric fields, the electron mobility in intrinsic GaAs is 0.86 m^2/Vs, about six times greater than that in silicon, 0.15 m^2/Vs. This is illustrated in Figure 2, showing the electron velocity versus electric field (v-E) relationship for both GaAs and Si. This high mobility was the reason for much of the early research and development of GaAs Field

Effect Transistors: the driving force was to increase the operating frequency of transistor devices.

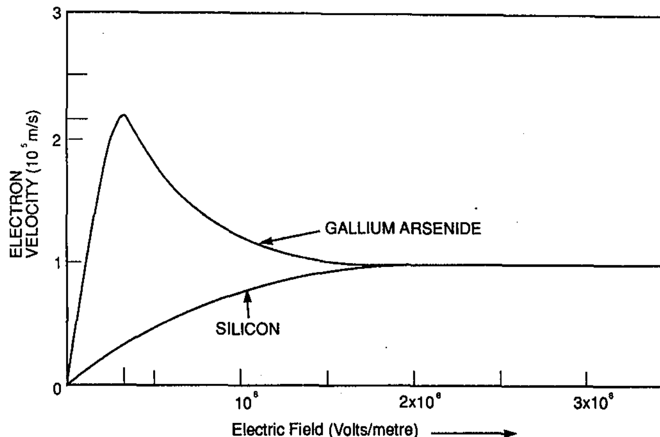

Fig.2. Comparison of the electron velocity — electric field characteristics for silicon and gallium arsenide.

Gallium arsenide exhibits the 'transferred electron' TE effect. This is an electric field-induced transfer of electrons from one region of the energy band structure to another, and results in a negative resistance being observed at microwave frequencies. The applications of the effect are as microwave oscillators and amplifiers: Transferred Electron Devices (TEDs). The structure and operation of these devices are explained later.

There has been a great deal of research and development of GaAs devices utilizing the above features, resulting in the widespread commercial application of TEDs, GaAs FETs and ICs, and LEDs and Lasers.

In recent years, there has been an upsurge of interest in structures and devices made from combinations of III–V compounds and III–V alloys: heterostructures. This began in the late seventies with the demonstration of enhanced electron mobility in the GaAs/AlGaAs heterostructure system [2]. This event also marked the advent of molecular beam epitaxy as a practical growth technique, bringing with it the possibility of making realizable heterostructure transistors and other devices with useful properties and characteristics, and improved performance over the straightforward GaAs devices. Some examples, which will be described in this paper, include: High Electron Mobility Transistor (HEMT); Heterojunction Bipolar Transistor (HBT); Double Heterojunction Laser; and new devices whose operation is based on quantum-mechanical principles.

Transferred Electron Devices

The v-E characteristics for gallium arsenide and silicon are shown in Fig. 2,

which illustrates the region of negative differential mobility (and hence resistance) present in GaAs. At low applied fields, the v-E relationship is linear for both materials, indicating that Ohm's law is being obeyed. Above some critical field in GaAs, it is clear that the Ohmic relation no longer holds: the electron velocity falls as the electric field is increased. This is due to the transferred electron effect, which was predicted by Ridley and Watkins [3] in 1961 for a semiconductor with a suitable band structure, and by Hilsum [4] in 1962 who showed that GaAs had such a band structure, as shown in Fig. 3.

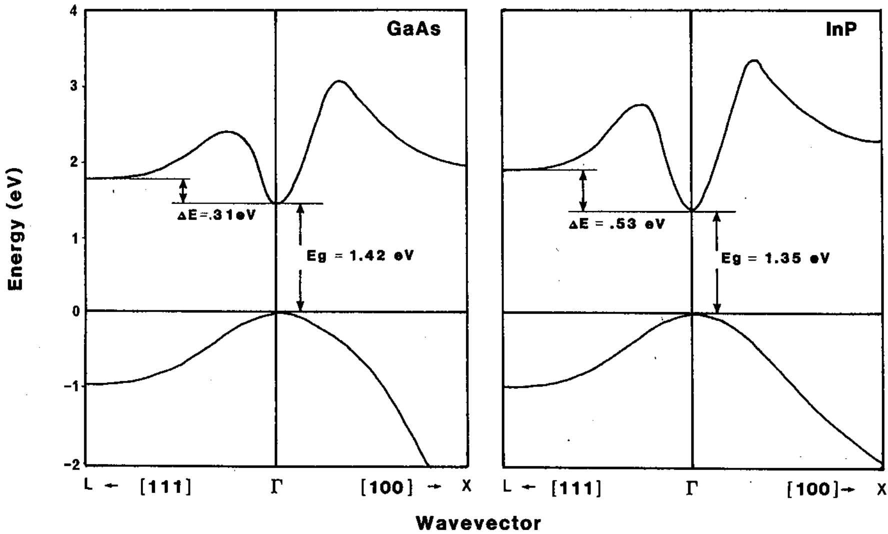

Fig.3. Energy band structures $\varepsilon(k)$ for GaAs and InP indicating the lower (central) valleys and the upper (satellite) valleys in the conduction band, used in the transferred electron process.

The conduction electrons are initially in the lowest energy valley, Γ minimum. Here, they are characterised by a low effective mass and have a high mobility. When the electric field is applied, these electrons are rapidly accelerated by the field to high velocities: they gain kinetic energy. The electrons can gain enough energy to transfer from this valley to the next higher valley, the L minimum. These upper valleys are characterised by a larger effective mass, and consequently both a lower electron mobility and a larger density of available electron states. The large density of states encourages transfer to these valleys of electrons with suitable energy. As the energetic electrons transfer to the upper valleys, the average velocity of all the electrons falls:

$$\text{average velocity } v = \frac{n_\Gamma v_\Gamma + n_L v_L}{n_\Gamma + n_L}$$

As the electric field increases and more electrons gain sufficient kinetic energy to transfer, so the average velocity continues to fall, until velocity saturation is attained, $v_{sat} \approx 10^5$ m/s.

It was the work of Gunn [5] in 1963 that provided experimental evidence for these theoretical models: thick samples of gallium arsenide and indium phosphide were subjected to short high voltage pulses, and microwave current oscillations were observed, at a frequency inversely proportional to the sample length. A threshold voltage (field) effect was noted for the onset of the oscillations. This result stimulated a great deal of research into the understanding and application of the transferred electron effect during the 1960's and 70's and the commercial development of transferred electron devices TEDs as microwave oscillators. A number of reviews of the transferred electron effect can be found in the literature [6–11].

TABLE I

	Indium Phosphide	Gallium Arsenide
Energy Gap E_g (eV)	1.33	1.43
$\Gamma - L$ separation E_s (Ev)	0.52	0.36
Effective mass Γ minimum	0.08 m_0	0.07 m_0
Effective mass L minimum	0.4 m_0	0.4 m_0
Low field mobility ($cm^2V^{-1}s^{-1}$)	4.750	8.000
Peak velocity ($\times 10^7$ cm s^{-1})	2.5	2.0
Peak to valley ratio	3.5	2.2
Treshold field (Kv cm^{-1})	10.0	3.2
Inertial energy time constant (ps)	0.7	1.5

Gallium arsenide and indium phosphide (InP) are virtually the exclusive choice of material for TEDs. The basic material parameters pertinent to the TE effect for these semiconductors is presented in Table I. The transferred electron device is a two-terminal structure as shown in Fig. 4: heavily n^+ doped contact and substrate regions are used to provide a low metal-to-semiconductor contact resistance, and sandwich the lightly n doped (10^{21} m^{-3}) 'active' region. TEDs commonly operate in a 'transit time' mode: that is, a high field region associated with an accumulation of transferred electrons is initiated at the cathode, travels along the length of the active region at the saturation velocity, and is collected at the anode where the electrons are discharged. A new accumulation is then formed at the cathode and the process repeats itself. The active region length is therefore inversely proportional to the operating frequency of the TED. The CW output power of GaAs and InP transferred electron oscillators as a function of frequency is shown in Fig. 5.

GaAs TEDs are the universal choice for operation at frequencies below about 40 GHz, with up to 1 W power available at 10–20 GHz. Low power applications include domestic intruder alarms, small boat marine radar systems, etc. InP is not practical for TEDs at these frequencies. The high threshold voltage and longer active region (for as given frequency) would mean that too large a voltage would need to be dropped across the active region, causing excessive power dissipation and

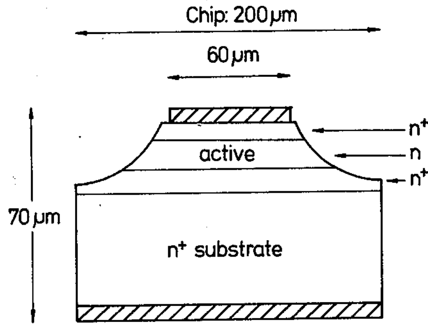

Fig.4. Structure of a GaAs Transferred Electron Device. The dimensions are typical of a low frequency, low power CW device.

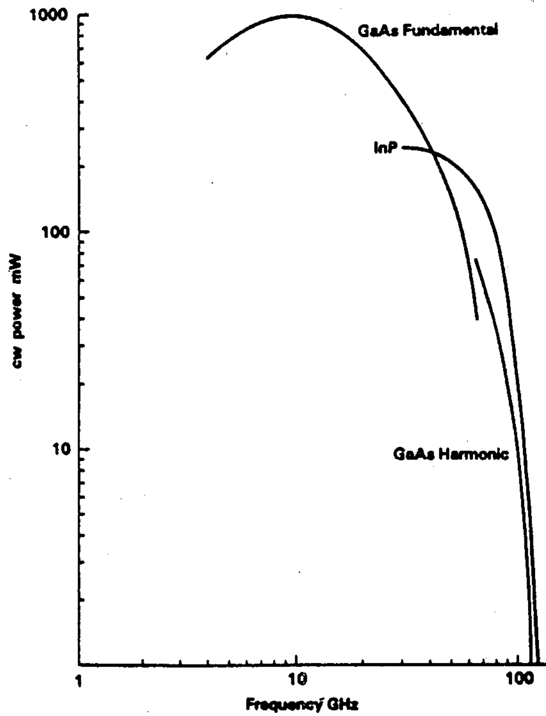

Fig.5. CW power output versus oscillation frequency for GaAs and InP TEDs.

device failure. InP is used for millimeter wave TE oscillators, from 60–110 GHz, where there is a need for portable and inexpensive microwave sources for personal communications systems.

TED oscillators can be operated in the second harmonic mode by reactively terminating the fundamental output with a suitable microwave circuit. GaAs TEDs are operated in harmonic mode to obtain useful microwave power at frequencies above about 65–70 GHz: 96 mW at 94 GHz has been observed. Useful power output up to 200 GHz has been obtained from InP devices operating in harmonic mode.

Pulsed operation is also possible, with peak powers of several hundred watts attainable. TEDs are well suited to situations such as medium range pulse Doppler radars, where low duty cycle operation is necessary. Again InP devices are used at higher frequencies than GaAs TEDs.

GaAs Field Effect Transistors

The GaAs MESFET (MEtal-Semiconductor FET) is the workhorse compound semiconductor microwave device today. It was developed in the late 1960's and it has been the subject of intense research activity in industry and academia worldwide since. Early GaAs FETs exhibited unity current gain cutoff frequencies f_T of a few GHZ, placing these devices firmly in the regime of microwave engineering. Modern GaAs FETs with gatelengths as small as 0.25 μm have been reported with an f_T of 126 GHz [12]. GaAs FETs also offer an advantage over TEDs in having three terminals, therefore naturally defining input and output ports, and so making amplifiers much easier to realise.

The GaAs MESFET structure is shown schematically in Fig. 6. As can be seen, this is both simple and in principle planar, lending itself to batch processing and integration. The essential feature of the device is the n-type layer which forms the channel between the Ohmic contacts at the source and drain. The conductance of the channel is modulated by the reverse bias voltage on the Schottky barrier gate contact.

Figure 6a shows a MESA type structure: the n-type layer is produced by epitaxial growth of high quality GaAs onto the SI substrate. This fabrication technique is generally used when the highest quality device material is required. The n-layer is etched away around the periphery of the device to provide electrical isolation. This clearly leaves a non-planar surface to the GaAs wafer and is undesirable from a processing point of view. An alternative means of isolation is to use ion bombardment (by hydrogen or oxygen, for example) to create damaged and nonconducting regions in the epitaxial layer between devices. This method retains the planar wafer surface. In Fig. 6b, a selectively ion-implanted FET structure is shown. In this fabrication technique the basic features of the FET are retained, but the Ohmic contact regions and the active channel are created by implanting directly into the SI substrate. This technique was pioneered by Rockwell [13] in 1978, giving them a world lead in GaAs FET IC technology at that time. It is generally used for digital GaAs FET integrated circuits for commercial applications, where cost is important and the expense of the epitaxial layer cannot be justified.

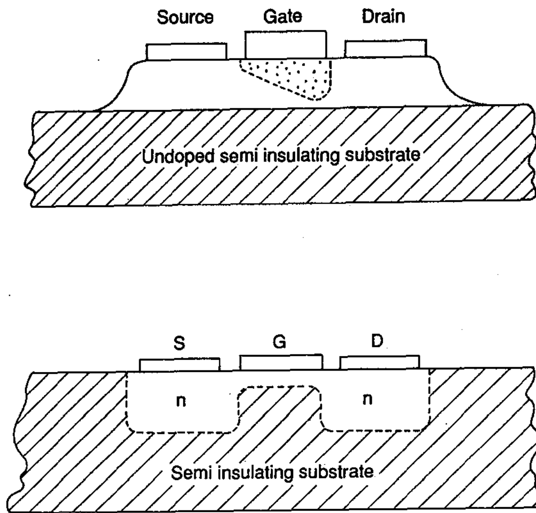

Fig.6. Structure of a GaAs MESFET: a) MESA device; b) selectively ion-implanted device.

The GaAs MESFET may naturally be compared with the silicon MOSFET. Whereas in MOS technology, the key advantage is that the conductance of the inversion channel is modulated through the insulating oxide by the gate bias, and no current flows in the gate, this is in contrast to the metal-semiconductor contact in the MESFET. No suitable oxide or dielectric has so far been found that can be used reliably in a device process in GaAs technology. However, as far as high frequency operation of the devices is concerned, GaAs MESFETs display some significant advantages over silicon MOSFETs:

- The 'channel mobility' of electrons in GaAs MESFETs can be up to ten times that seen in silicon MOSFETs in strong inversion. This is due to the high electron velocities in the channel region, possibly as a result of velocity overshoot effects, and results in much reduced transit times in GaAs FETs.
- The high electron mobility at low electric fields in GaAs also brings about an improvement, in a subtle way. Movement of the electrons from the source contact region to the entrance of the active channel constitutes a parasitic resistance: the access resistance. The high electron mobility in GaAs reduces this series resistance and improves gain and noise performance at high frequencies. Ways by which even the small access resistance can be reduced have been investigated: 'self-alignment' techniques where the gate metallisation and the heavily-doped source and drain regions are automatically registered in abutment, thus largely eliminating the source-to-channel resistance. Two basic methods have been used:
  - SAINT technique [14], where the Ohmic contacts are placed first, and

the gate aligns to them;

- o Stable-gate technology, where the Schottky gate metal is used as the source-drain implant mask. This places stringent requirements on the thermal stability of the gate metallisation; refractory metals are often used [15].

- The MESFET channel is isolated by the relatively thick semi-insulating substrate. This reduces parasitic interdevice capacitances and is important for the high frequency performance of the device.

Discrete GaAs MESFETs have found application as both low noise and power amplifiers at microwave frequencies. Noise figures as low as 0.56 dB at 16 GHz have been reported [16], although as LNAs, GaAs FETs are becoming overshadowed by the performance of heterojunction FET devices (see Fig. 7).

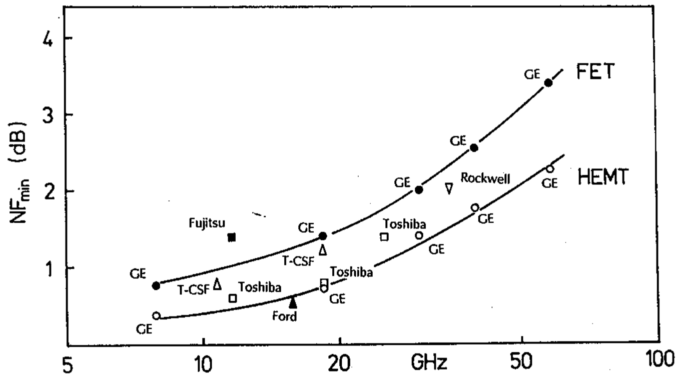

Fig.7. Comparison of the minimum noise figures NF_{min} of GaAs FETs and GaAs/AlGaAs HEMTs. All devices have a 0.25 μm gatelength.

Gallium Arsenide Integrated Circuits

While GaAs IC designs have been reported by research laboratories for several years [17], it is only relatively recently that GaAs substrate material of sufficiently high quality — in terms of stoichiometry, defects and impurities, thermal and mechanical stability — has become available, thus making possible the large scale production and application of GaAs ICs on a commercial basis. Both digital and analogue (monolithic microwave) ICs are produced. The current commercial GaAs IC vendors include some of those companies who originally set up fabrication facilities for in-house consumption, and also newcomers to the marketplace in the form of 'GaAs IC foundries'. The vendors may hire their design rules and fabrication technology to the customer for ASIC design and manufacture, as well as producing standard parts.

Commercial analogue MMICs are commonly amplifiers and switches, used in modulator applications. Recent reviews cover a number of applications of MMICs in communications systems [18, 19], including novel applications such as frequency converters and receiver chips [20]. Digital ICs are mostly multiplexer/demultiplexers, frequency dividers and a wide range of 'standard' logic gates, operating at clock rates of typically between 1 and 7.5 GHz [21]. Microprocessor and RAM functions are also available [21]. With such a variety of GaAs IC products available, both commercially and in-house, it is no surprise that they are finding their way into a number of commercial microwave and high speed time-domain test instruments, where the decision to use a GaAs IC is made to yield a price/performance advantage [22].

Heterostructures and Band Gap Engineering

The GaAs MESFET and associated integrated circuits have played a crucial role in the development of many aspects of GaAs semiconductor technology, by offering a standard of performance and acting as a vehicle for new technology developments. There has been particularly rapid progress in recent years in the sophisticated crystal growth techniques of molecular beam epitaxy MBE and metallorganic chemical vapour deposition MOCVD. These techniques allow the epitaxial growth of III–V semiconductor layers with great control over the purity, doping and thickness, and also allow the growth of alloys of III–V semiconductors with control over the mole fraction of the alloy constituents. Atomically abrupt interfaces between regions of different alloy and doping can be achieved. Such technological features were first exploited in the modulation-doped GaAs/AlGaAs heterojunction system to demonstrate enhanced electron mobility [2]. This virtually atomic level of control over the semiconductor material properties, permitting precise definition of the band structure, has opened up enormous possibilities for the device engineer: Band Gap Engineering.

High Electron Mobility Transistors

The HEMT, or MODFET (modulation-doped FET), is a very close relative of the GaAs MESFET, sharing the same geometry. The HEMT has extended useful FET performance to over 100 GHz. The speed of the MESFET is limited by (among other things) the mobility and the number of electrons in the channel region. At high doping levels, the mobility falls: for typical doping of 10^{23} donors/m^3, the electron mobility may be about 0.4 m^2/Vs, less than half the intrinsic value. The HEMT uses a heterostructure which cleverly allows large densities of electrons in the channel, and at the same time a high mobility, by physically separating the electrons from the scattering effects of their host donors.

The principle of the device is illustrated in Fig. 8, which shows an heterojunction between an undoped GaAs layer and heavily n-type AlGaAs layer: this is a type I heterojunction, the AlGaAs being the wide gap material. In equilibrium the heterojunction relaxes to the form shown in Fig. 8. A narrow potential well forms

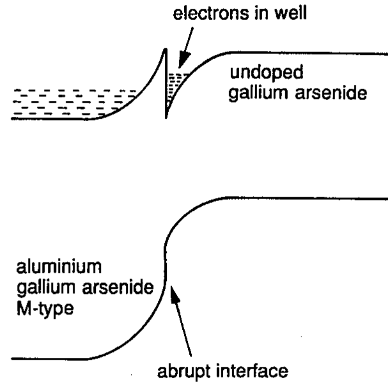

Fig.8. Energy band structure of an n-AlGaAs/undoped GaAs heterojunction, showing the electrons filling the conduction band notch at the interface.

in the GaAs at the interface, and some electrons from the AlGaAs fall into this well, leaving a depletion region in the AlGaAs adjacent to the junction. The result is that a thin channel is formed in the undoped GaAs, containing a high density of electrons. This undoped region has a high electron mobility associated with it, and so we have the combination of high electron density and high mobility: a high speed device. In practical devices an undoped AlGaAs 'spacer' layer of about 5 nm thickness is placed at the interface to further separate the electrons from the influence of the scattering by the ionised donors. The absence of ionised dopant scattering is particularly apparent at low temperatures, where electron mobilities in excess of 100 m^2/Vs have been obtained.

The HEMT device structure is shown schematically in Fig. 9. The similarities with the MESFET are clearly evident. The high electron density and mobility in the channel lead to high frequency operation, with f_T over 100 GHz. The HEMT also exhibits good low noise behaviour, as a result of the reduced scattering in the channel. Figure 7 shows the noise performance advantage of 0.25 μm gatelength GaAs/AlGaAs HEMTs over conventional GaAs MESFETs of similar dimension. The current 'best' performance is a minimum noise figure of 2.2 dB at 60 GHz, and only 0.4 dB at 8 GHz with 15 dB of associated gain [23]. HEMT ICs have also been made, using similar architectures and layouts to GaAs FET ICs. The HEMT circuits show shorter propagation delay times than GaAs FET circuits in general. Complex circuits including 8x8 and 16x16 multipliers and 4 K RAMs have been built in research laboratories [24].

Other III–V heterojunction systems have been studied in HEMT applications. In particular, the use of InGaAs alloy as the channel material has promise: intrinsic InAs has a high electron mobility of over 1.2 m^2/Vs at room temperature, and so an improvement in performance over GaAs channel HEMTs may be expected.

Unfortunately, InAs is not lattice matched to GaAs, and so to use InAs in a GaAs-based HEMT, the InAs mole fraction in the InGaAs alloy of the channel

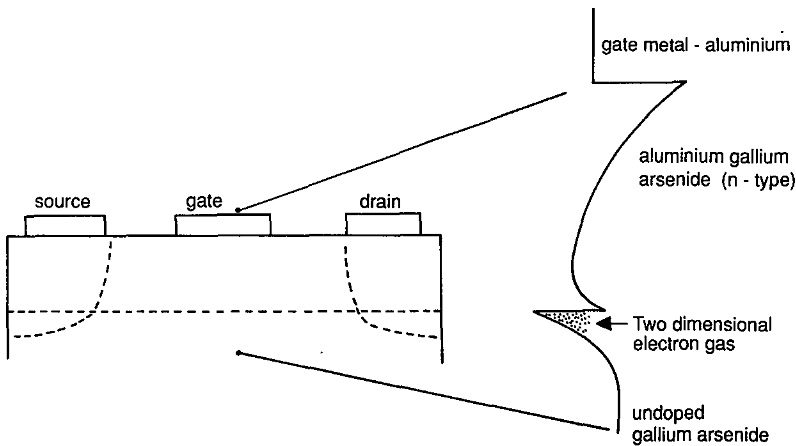

Fig.9. HEMT device structure, showing the location of the electron channel.

layer must be kept small, usually between 15 and 25 %, to minimize the mismatch. This also limits the mobility improvement that may be obtained. The InGaAs layer grows on the GaAs substrate with built-in strain: the InGaAs lattice is stretched to fit onto the host GaAs. Provided the layer is thin this strain can be accommodated without the generation of dislocations which would severely hamper the device performance. This structure is known as a *pseudomorphic* HEMT. The confining layer is AlGaAs, as before. This device has outperformed both GaAs MESFETs and conventional HEMTs at frequencies up to 60 GHz, and has recently shown itself to be a candidate for W-band (75–110 GHz) systems [25]. The following GE device results are among the current 'best' performers:

InAs mole fraction = 25%

(a) gatelength = $0.15\,\mu m$ (from [26])

f_T = 135 GHz
NF_{min} = 1.8 dB @ 60 GHz, Associated gain = 6.4 dB
NF_{min} = 0.55 dB @ 18 GHz, Associated gain = 15.2 dB

(b) gatelength = 80 nm (from [27])

NF_{min} = 1.9 dB @ 60 GHz, Associated gain = 9.2 dB
NF_{min} = 0.7 dB @ 18 GHz, Associated gain = 14.1 dB

Further improvements in the performance of InGaAs channel HEMTs can be obtained by increasing the InAs mole fraction. To do this, InAlAs/InGaAs structures lattice-matched to InP can be used. This InP-based lattice-matched HEMT is thought to be superior to the GaAs-based pseudomorphic HEMT for millimeter wave low noise applications for the following reasons:

(a) a large sheet electron density is obtained in the channel, since the band gap discontinuity is greater and the doping efficiency of Si in InAlAs is high;

(b) better carrier confinement in the channel as a result of the band structure;

(c) higher electron mobility and peak velocity in the channel due to higher mole fraction of InAs (up to about 50 %).

These properties increase the device transconductance, maximum frequency of oscillation, and current gain cutoff frequency, and reduce the noise figure. Excellent noise performance up to W-band has been reported for these HEMTs:

NF_{min} = 0.3 dB @ 18 GHz with 17.2 dB of associated gain, and
NF_{min} = 1.4 dB @ 93 GHz with 6.6 dB of associated gain, with
f_T ≈ 160 GHz, for 0.15μm gatelength devices.

These HEMTs would seem to be candidates for applications in InP-based integrated optoelectronic systems.

Heterojunction Bipolar Transistors

In a conventional (homojunction) bipolar transistor, a high current gain is achieved by the simultaneous use of a large doping asymmetry between the heavily doped emitter and the lightly doped base, and a very narrow base to minimize recombination in this region. To a first approximation the current gain is given by the ratio of majority to minority current across the emitter-base junction, which in turn is given by the doping ratio. Unfortunately, the low base doping and its narrow width yield a large base resistance which degrades the transistor's high frequency performance. Consequently, there is seen to be a trade-off between frequency and current gain, according to the application.

Improvements to this basic transistor structure were outlined by Shockley in his original patent in the form of a wide band gap heterojunction emitter; this device has been described theoretically by Kroemer [28]. The desired effect of a wide band gap heterojunction emitter is to provide a greater potential hill for the minority carriers flowing from base to emitter, than for the majority carriers flowing from emitter to base, thereby increasing the available gain. Figure 10 shows a simple band diagram for an *n-p-n* GaAs/AlGaAs HBT. The potential hill for holes flowing from base to emitter is greater than the electron potential from emitter to base, by $\Delta\varepsilon \approx 0.25$ eV. This difference in potential can be shown to increase the current gain β by a factor $\exp(\Delta\varepsilon/kT)$. At room temperature ($kT = 0.025$ eV), this yields an increase of 22 000 times! In practice, this remarkable improvement is traded-off against increases in the base doping of several orders of magnitude. This has two related effects:

1. it reduces the base resistance, improving high frequency performance;

2. it allows the base width to be made narrower without significantly increasing its resistance, thus reducing the base transit time and again improving high frequency performance.

The base doping may exceed that in the emitter, yet high current gains can still be achieved.

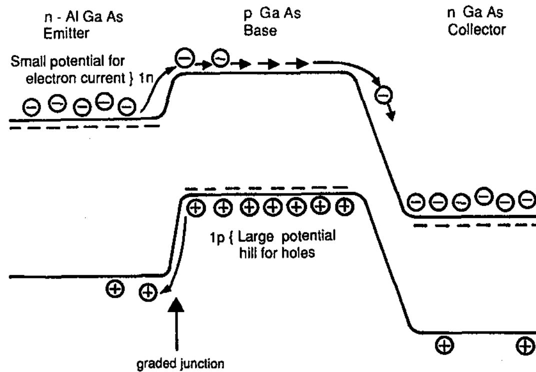

Fig.10. Energy band structure of a GaAs/AlGaAs graded heterojunction bipolar transistor, illustrating the increased potential hill for minority hole flow from the base to the emitter.

In the GaAs/AlGaAs heterojunction, the 'notch' in the conduction band seen in HEMTs is undesirable in this context, and can be avoided by the use of a graded junction: the mole fraction of Al is increased from zero to the desired quantity (about 25 %) over a small distance. The high valence band potential hill is retained.

In comparison with GaAs MESFETs, HBTs offer the following advantages: higher transconductance, higher current and power density, better threshold voltage matching, lower demands on fine-line lithography for high frequency operation, and control over the breakdown voltage. One drawback is a result of the vertical structure of the HBT: electrical contact to the various regions of the device requires careful and controlled etching. Selective plasma etching techniques can be used for GaAs/AlGaAs devices. Nonetheless, a non-planar structure results.

The basic figure of merit for the HBT is the unity current gain frequency f_T. GaAs/AlGaAs HBTs have been widely studied: Fig. 11 illustrates the improvements in f_T that have been achieved by several groups over the past decade or so. The current best performance is $f_T = 105$ GHz, by a NTT device [29].

Analogue device performance compares well with GaAs MESFETs: a minimum noise figure of 2 dB at 16 GHz with a 10 dB associated gain has been reported [30]. High speed digital devices and circuits have also been made: a CML divide-by-4 circuit operating at 26.9 GHz; a yield of 87 % on circuits operating above 20 GHz was achieved with these devices [30]. A remarkable achievement in HBT technology is the Texas Instruments 32-bit microprocessor containing 12,900 equivalent NOR gates and operating at over 100 MHz clock speed [31].

As with HEMT devices, other III–V semiconductor heterojunction systems can be used. Very promising high frequency performance has been demonstrated by the InGaAs/InP lattice-matched systems: f_T of 165 GHz. This would indicate possible applications in InP-based integrated optoelectronic ICs.

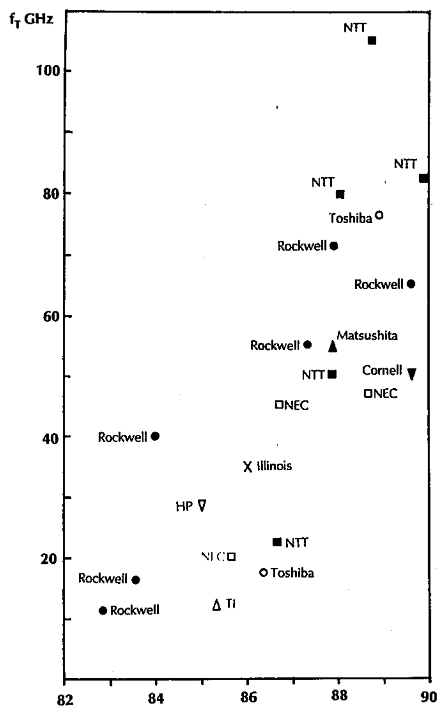

Fig.11. Improvements in the HBT cutoff frequency.

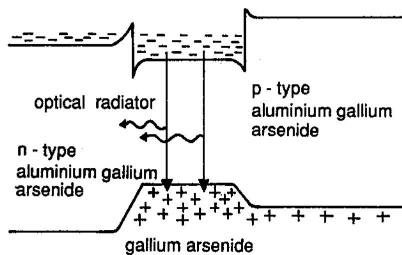

Fig.12. Energy band diagram of a Double Heterojunction Laser.

Lasers

As outlined previously, the direct bandgap in GaAs and other III–V semiconductors enables radiative recombination of electrons and holes to take place: i.e. the emission of light. A GaAs *p-n* junction in forward bias can be used for light emission, as in LED and Laser devices. High densities of carriers are injected over the barrier into the depletion region, producing favourable conditions for recombination. In the laser device, the ends of the chip are polished plane parallel so that the generated photons are largely reflected back into the device itself; these photons then stimulate further recombination and produce laser action. The simple *p-n* device suffers from some drawbacks:

- the light is not well confined, so intensities can be low;
- a large forward bias current density, of the order of 10^9 A/m^2, is required before the onset of laser action. Under these conditions the device is heavily stressed, leading to reduced lifetime in practical situations.

More efficient laser action can be achieved by confining the charge carriers in a narrow-gap semiconductor, between two potential barriers at heterojunction interfaces. This device is the Double Heterojunction Laser: the operation of a GaAs/AlGaAs device is shown in Fig. 12. The laser action is due to radiative recombination in the thin GaAs region: the injected electrons and holes cannot move back into the AlGaAs because of the potential barriers. Threshold current densities below 10^7 A/m^2 have been achieved with these devices. An added advantage is one of confinement of the emitted light due to the difference in dielectric constant between GaAs and AlGaAs.

When the width of the potential well formed by the heterojunctions is reduced to below about 50 nm, then size quantization occurs in the well, resulting in the appearance of discrete energy levels for the electrons and holes in the well. The energies of the levels are related to the quantum well width: the narrower the well, the greater the separation between the levels. This is illustrated schematically in Fig. 13. Radiative transitions can now be made between these quantized levels, and consequently a very narrow linewidth results, desirable for monomode fibre applications. This structure is the basis of the Quantum Well Laser: the device can consist of one or many quantum wells. These lasers present a range of new opportunities for integrated optoelectronic systems.

Quantum Well Devices

The quantum well QW and multiple quantum well MQW laser structures outlined above are examples of devices that are now being made, researched and used, which employ quantum mechanical effects as integral features of their operation. A whole range of such devices may be envisaged, and some have been recently proposed by Capasso [32]. The basis of many of these devices is quantum confinement between two heterojunction barrier layers: a double barrier device. The fundamental application of double barrier devices is in the Resonant Tunneling Diode.

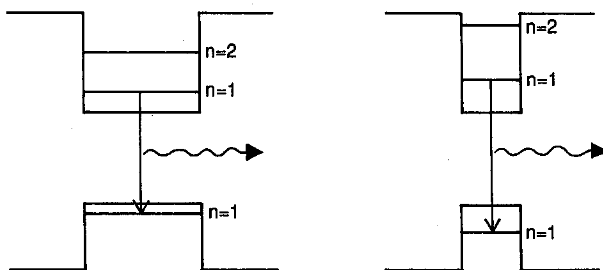

Fig.13. Illustration of how the width of the double heterojunction well affects the energy levels in the well, and consequently the wavelength of the emitted radiation.

Resonant Tunneling Diode

The basic structure of the Resonant Tunneling Diode is illustrated by the conduction band diagram in Fig. 14a. A thin GaAs layer is sandwiched between two AlGaAs layers as in the QW laser, but now the barrier layers are also made extremely thin. The whole structure is furnished with metal contacts to the AlGaAs barriers, as shown. When an electric field is placed across the contacts, the band structure takes on the form shown in (b). The current-voltage characteristics for the device are shown in (c). For very small applied voltages the resistance of the structure is large. As the voltage increases, the electrons in the left-hand contact become equal in energy with those electrons at the energy level E_1 in the quantum well. Quantum mechanical tunneling through the AlGaAs barrier can now take place as the tunneling electrons have energy states available to them. The tunneling proceeds through the second barrier to the other contact. The resistance of the structure falls dramatically at this specific applied voltage, and the current through the structure shows a large peak. As the voltage is further increased, the contact is no longer coincident with E_1, and so the current falls. Thus, the device shows a differential negative resistance characteristic (even at room temperature).

Resonant tunneling through double barriers was first observed by Chang et al. in 1974 [33], but the observed negative differential resistance was thought to be too small for device applications. More recent results have shown that oscillation frequencies in excess of 400 GHz can be achieved [34], with output power of the order of μW: this is sufficient for local oscillator applications in infra-red/millimeter wave receivers at these frequencies. Recent reviews of resonant tunneling diodes cover the basic physics as well as *dc* and high frequency applications [35, 36].

The resonant tunneling concept can be applied to more conventional devices. An example is the Quantum Well Injection Transit Time device QWITT. The tunneling structure is used to inject current pulses into a transit time device similar to an IMPATT [37]. By using tunneling instead of an avalanche process for injection, there is some loss of efficiency, but there is a compensating reduction in noise. These devices again operate as oscillators at several hundred GHz.

In addition to the two terminal devices, three terminal structures have been

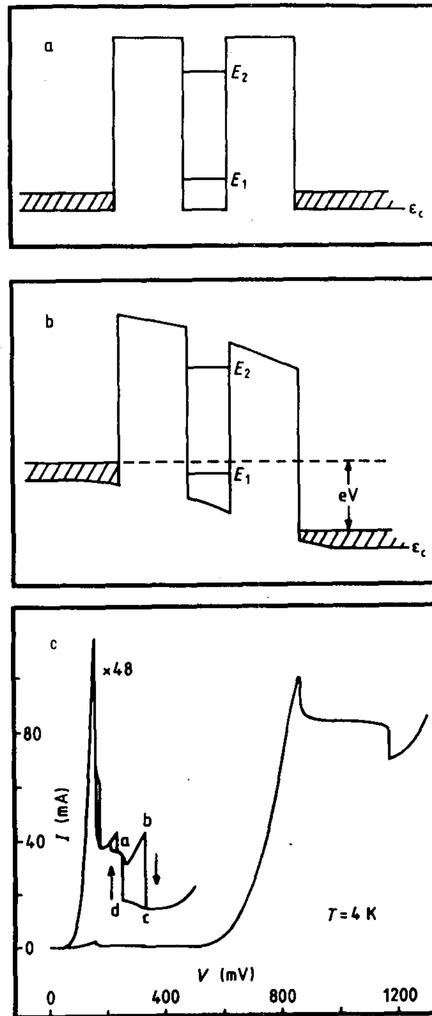

Fig.14. Conduction band structure of a GaAs/AlGaAs Resonant Tunneling Diode: a) without electrical bias; b) bias voltage applied; c) current-voltage characteristics showing negative differential resistance.

proposed and developed by Capasso and co-workers [32]. Resonant Tunneling Bipolar Transistors RTBT have been shown to act as efficient frequency multipliers, producing fifth-harmonic output from a 350 MHz input at 15 % conversion efficiency, and as functional logic elements greatly reducing the gate count [32].

Conclusions

Gallium arsenide and its related III–V compounds have now established themselves as materials for devices and circuits for current and developing engineering applications. These materials are not usurping the role of silicon but creating new markets in key communications and IT areas where silicon cannot perform. Significant future developments are indicated for GaAs and related compounds, in terms of technological progress in the development of existing devices and integrated systems, and also in the potential new quantum well devices currently being researched throughout the world.

References

[1] J.S. Blakemore, *J. Appl. Phys.* **53**, R123 (1982).

[2] R. Dingle, H.L. Stormer, A.C. Gossard, W. Wiegmann, *Appl. Phys. Lett.* **33**, 665 (1978).

[3] B.K. Ridley, T.B. Watkins, *Proc. Phys. Soc.* **78**, 293 (1961).

[4] C. Hilsum, *Proc. IRE* **50**, 185 (1962).

[5] J.B. Gunn, *Solid State Comm.* **1**, 88 (1963).

[6] H. Kroemer, *Proc. IEEE* **52**, 1736 (1964).

[7] J.E. Carroll, *Hot Electron Microwave Generators,* Edward Arnold, 1970.

[8] P.J. Bulman, G.S. Hobson, B.S. Taylor, *Transferred Electron Devices* Academic Press, 1972.

[9] B.G. Bosch, R.W.H. Engelmann, *Gunn Effect Electronics,* Wiley, 1975.

[10] M.P. Shaw, H.L. Grubin, P.R. Solomon, *The Gunn-Hilsum Effect,* Academic Press, 1979.

[11] D.M. Brooksbanks, in *Microwave Solid State Component and Subsystem Design*, eds. D.V. Morgan, M.J. Howes, R.D. Pollard, Leeds University Press, 1983.

[12] G.W. Wang, M. Feng, *IEEE Electron Device Lett.* **10**, 386 (1989).

[13] R.C. Eden, B.M. Welch, R. Zucca, *ISSCC Conf. Dig.*, p.68 (1978).
B.M. Welch et al., *IEEE Trans. Electron Devices* **27**, 1116 (1980).

[14] K. Yamasaki et al., *Jpn. J. Appl. Phys. Suppl.* **22**-1, 381 (1982).

[15] D.V. Morgan, J. Wood, *Appl. Surf. Sci.* **38**, 517 (1989).

[16] G.W. Wang et al., *IEEE Electron Device Lett.* **10**, 186 (1989).

[17] see *Proceedings of GaAs IC Symposium* 1981 onwards.

[18] D. Maki, in *Gallium Arsenide: Materials, Devices and Circuits,* eds. M.J. Howes, D.V. Morgan, Wiley, 1985.

[19] D.R. Decker, in *VLSI Electronics*, eds. N.G. Einspruch, W.R. Wisseman, Academic Press 1985.
[20] see 'Special Issue on MMICs', *IEEE Trans. Microw. Theory Tech.* **35** (1987).
[21] J. Browne, *Microw. RF* **27**, 139 (1988).
[22] V. Peterson, *Microw. J.* (August 1989) p. 46.
[23] K.H.G. Duh et al., *IEEE Trans. Electron Devices* **35**, 249 (1988).
[24] M. Abe et al., *IEEE Trans. Electron Devices* **36**, 2021 (1989).
[25] P.C. Chao et al., *Electron. Lett.* **25**, 504 (1989).
[26] M-Y.Kao et al., *IEEE Electron Device Lett.* **10**, 580 (1989).
[27] P.C. Chao et al., *IEEE Trans. Electron Devices* **36**, 461 (1989).
[28] H. Kroemer, *J. Vac. Sci. Technol. B* **1**, 126 (1983).
[29] T. Ishibashi et al., *IEEE Trans. Electron Devices* **35**, 401 (1988).
[30] P.M. Asbeck et al., *IEEE Trans. Electron Devices* **36**, 2032 (1989).
[31] D.A. Whitmire, V. Garcia, S. Evans, *ISSCC Conf. Dig.,* p.34 (1988).
[32] F. Capasso et al., *IEEE Trans. Electron Devices* **36**, 2065 (1989).
[33] L.L. Chang, L. Esaki, R. Tsu, *Appl. Phys. Lett.* **24**, 593 (1974).
[34] E.R. Brown, T.C.L.G. Sollner, C.D. Parker, W.D. Goodhue, C.L. Chen, *Electron. Lett.,* in press.
[35] E.R. Brown, T.C.L.G. Sollner, W.D. Goodhue, C.L. Chen, in *Proc. SPIE - Int. Soc. Opt. Eng.* **943**, 2 (1989).
[36] F. Capasso et al., in *Submicron Integrated Circuits*, ed.R.K. Watts, Wiley, 1989.
[37] V.P. Kesan, *IEEE Electron Device Lett.* **8**, 129 (1987).